JOURNAL OF CHEMICAL INFORMATION AND MODELING

ARTICLE

pubs.acs.org/jcim

Comparison of Virtual High-Throughput Screening Methods for the Identification of Phosphodiesterase-5 Inhibitors

Sanna P. Niinivehmas,[†,§] Salla I. Virtanen,[†,§] Jukka V. Lehtonen,[‡] Pekka A. Postila,[†,∥] and Olli T. Pentikäinen*[,†]

[†]Department of Biological and Environmental Science, P.O. Box 35, FI-40014 University of Jyväskylä, Finland

[‡]Department of Biosciences, Biochemistry, Åbo Akademi University, Tykistökatu 6A, FI-20520 Turku, Finland

Supporting Information

ABSTRACT: Reliable and effective virtual high-throughput screening (vHTS) methods are desperately needed to minimize the expenses involved in drug discovery projects. Here, we present an improvement to the negative image-based (NIB) screening: the shape, the electrostatics, and the solvation state of the target protein's ligand-binding site are included into the vHTS. Additionally, the initial vHTS results are postprocessed with molecular mechanics/generalized Born surface area (MMGBSA) calculations to estimate the favorability of ligand-protein interactions. The results show that docking produces very good early enrichment for phosphodiesterase-5 (PDE-5); however, in general, the NIB and the ligand-based screening performed better with or without the added electrostatics. Furthermore, the postprocessing of the NIB screening results using MMGBSA calculations improved the early enrichment for the PDE-5 considerably, thus, making hit discovery affordable.

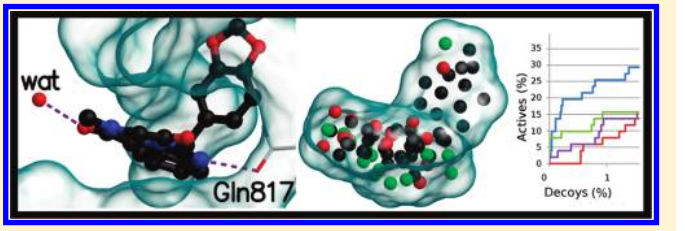

INTRODUCTION

Rational drug development requires efficient ways to screen active molecules from massive molecular databases. This task has traditionally been approached by ligand-based or protein structure-based virtual high-throughput screening (vHTS) methods. Molecular docking is a protein structure-based method that samples through various ligand conformations in relation to the ligand-binding pocket of the target protein. The drawback is that the docking procedure is computationally laborious and time-consuming. Also various studies suggest that the docking scoring functions do not always distinguish active ligands from inactives and therefore the docking results are case-specific.[1−4] The ligand-based methods either compare the shape of the known ligands or their chemical properties against the compounds in the molecular databases. The ligand-based methods depend heavily on the assortment of the known active ligands and, therefore, there has to exist potent ligand(s) to accomplish successful vHTS. In pharmacophore modeling the structural data of the ligand and the protein crystal structure can be combined, but the model creation can be a lengthy and complex process.[5]

There is another viable protein structure-based vHTS method, negative image-based (NIB) screening, that shows great promise.[2,6,7] A negative image of the ligand-binding site is created, and the shape of this ligand-like entity (or NIB model) is then compared against compounds in the molecular databases. We have earlier shown that these simple space-filling NIB models of the ligand-binding pockets work well in vHTS for a multitude of targets.[2] The NIB method was better at finding active compounds than docking, and in many cases it worked better than the ligand shape-based method. The use of multiple crystal structures or molecular dynamics (MD) simulation snapshots could also enhance the yield of the NIB searches.

Although the simple shape-based NIB models of the ligand-binding pockets worked satisfactorily in most cases,[2] there was potential to improve the method even further by introducing novel features into the vHTS protocol. First, our aim was to enhance the success rate of the shape-based NIB method by adding electrostatic information directly into the negative images. Second, as the ligand binding is in many cases affected by water molecules we wanted to consider the significance of solvent when building the NIB models. Third, we wanted to increase the enrichment of the initial vHTS searches by introducing additional steps that would estimate the favorability of the ligand-protein interaction (or ligand-binding affinity). In practice, the free energies involved in ligand binding can be estimated by combining MD simulations and molecular mechanics/generalized Born surface area (MMGBSA[8]) calculations. Although these additional steps increase the computational costs of the searches, they should also improve the success rate of the vHTS methods dramatically if only the top ranked results are rescored/postprocessed.

In our previous study we optimized the NIB screening for example with nuclear receptors, whose ligand-binding pockets are lipophilic.[2] In this study the efficiency of vHTS methods was tested using cyclic nucleotide phosphodiesterase-5 (PDE-5) as

Received: November 18, 2010
Published: May 19, 2011

dx.doi.org/10.1021/ci1004527 | J. Chem. Inf. Model. 2011, 51, 1353–1363

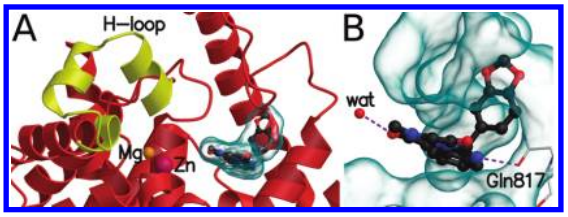

Figure 1. The substrate-binding site of PDE-5 catalytic domain. (A) The 3D structure of PDE-5 with bound tadalafil that is shown with ball-and-stick and surrounded by transparent water-accessible surface. The H-loop that is adjusted during PDE5-I binding is highlighted in yellow. (B) The key binding interactions of tadalafil include hydrogen bonds with the side chain Gln817 and one water molecule (wat). The hydrogen bonds are depicted by dashed lines (magenta). The lipophilic surfaces of the PDE-5 residues that complement the shape of the tadalafil are shown with transparent water-accessible surface.

the target protein (Figure 1A). The PDE-5 was an ideal target to improve the NIB screening with electrostatic information, because its substrate-binding site contains both polar groups and coordinated water molecules (Figure 1B). The PDE-5 regulates intracellular concentrations of second messenger cyclic guanosine 5′-monophosphate (cGMP) through hydrolyzation reactions. Moreover, the catalytic domain of PDE-5 has also been crystallized in complex with various PDE-5 inhibitors (PDE5-Is[9−13]). The crystallography suggests that PDE5-I binding promotes enclosure of the substrate-binding site as the H-loop adjusts in relation to the bound inhibitor (Figure 1A). The PDE5-I binding blocks competitively the substrate from binding to the enzyme, and, thus, the catalytic reaction is inhibited.[10] Potent PDE5-Is such as vardenafil (Levitra, sold by Bayer Corp./GSK Corp.), sildenafil (Viagra, Pfizer Corp.), and tadalafil (Cialis, Eli Lilly Corp.) are nowadays the preferred choice in treating male erectile dysfunction.[14] However, the PDE5-Is also alleviate the symptoms of e.g. idiopathic pulmonary hypertension,[15] arterial problems,[16−18] and premature ejaculation.[19]

In short, the aim of this study was to compare the ligand-shape and the protein structure-based vHTS methods using the catalytic domain of PDE-5 as a model system. We also wanted to improve the NIB screening by introducing electrostatic information from the protein structure into the searches. Moreover, the top 5% of the ranked results were rescored with the MD/MMGBSA protocol to estimate the free energy change upon binding. The effects of electrostatics were also tested using other target proteins that we have studied in our recent work.[2] The results show that the NIB screening protocol can be easily employed to the identification of PDE5-Is from molecular databases, and it should be applicable to other target proteins as well.

MATERIALS AND METHODS

Ligand and Protein Structures. The 3D structures of the PDE-5 catalytic domain were acquired from the Protein Data Bank (PDB).[20] TLEAP in ANTECHAMBER 1.27[21] was used to add hydrogens into the protein structures. The active ligands and decoy molecules were compared against the 3D structures of the tadalafil and sildenafil extracted directly from the PDE-5 crystal structures (PDB: 1XOZ[12] and 2H42,[10] respectively) in the ligand-based vHTS. Both the active compounds (n = 51) and decoys for the PDE-5 were acquired from the Directory of Useful Decoys (DUD).[22] The PDE-5 specific decoys are referred to as PDE-5 decoys (n = 1807). In addition, the other DUD ligand-sets (n = 2942; hereafter called DUD decoys) were used as an additional decoy set. Unfortunately, the effects on the PDE-5 function have not been determined for molecules in either decoy set. The decoy set that combines both the PDE-5 decoys and other DUD decoys is referred to as the PDE-5/DUD decoys (n = 4749). The DUD decoys were included to make the early enrichment studies more reliable. Low energy conformers and electrostatics of the molecules were generated using the Schrödinger ConfGen[23] routine with Merck molecular force field (MMFF94[24]). From the predefined protocols in ConfGen the Fast option was employed for conformational searching.

Negative Image Creation. Negative images of the PDE-5 substrate-binding site were derived using the 3D structural data provided by the PDE-5 crystal structures with bound inhibitor molecules.[10,12] The number of water molecules that were left into the ligand binding cavity was varied, and several solvation models were tested. However, the results are shown for only two NIB solvation models (NIB-SM1 and NIB-SM2) whose composition (shape and charge) and subsequent results diverged substantially from each other. Both NIB models have additional points at the bottom of the substrate binding site, which are not replaced by bound tadalafil, sildenafil, or vardenafil. The NIB-models were generated with VOIDOO/FLOOD[25] using modified parameters as described earlier.[2] For other targets, the previously calculated NIB-models were used.[2]

Shape Comparison and Electrostatic Information. The shape comparison of the NIB models or the bound ligands seen in the crystal structures against the ligand/decoy sets was accomplished using SHAEP[26] as explained in our preceding study.[2] The searches were done either with only the shape of the NIB model or the compound, i.e. with 'onlyshape' option in SHAEP, or with both the shape and the electrostatics. For electrostatic potential comparisons, MMFF94-charges were used for all small molecules. The electrostatic information for the proteins were assigned as atom-centered MMFF94-charges.[24] The protein charges were then used to create opposite charges for the data points in the NIB model. The charges of the protein atoms within 2.7 Å radius of each of the NIB model data points were averaged, and the opposite number of that charge was assigned to the corresponding NIB data point. This radius takes into consideration the atoms within hydrogen bonding distances and other relevant charges in the substrate-binding site. In the shape comparison, the ligand or the NIB model structures were used either individually or they were combined, and only the best result was used when ranking the combined runs. The accentuation of electrostatic potentials and shape was optimized by varying their contributions in 0.05 intervals. The enrichment was highest, when the shape and the electrostatics of the substrate-binding were contributing equally (0.5 ± 0.1; data not shown). Similarly, other parameters associated with the electrostatic potentials, e.g. the radius of electrostatic potentials and shape density with partial charge weighting, were studied, but none of them had significant influence to the enrichment (data not shown), and, accordingly, the default parameters were used.

Docking. The molecules were used for docking as provided within the DUD.[22] The docking was performed with the tadalafil-(PDB: 1XOZ) and sildenafil-bound (PDB: 2H42) PDE-5 crystal structures. The protein structures were prepared with the Protein Preparation Wizard in MAESTRO.[27] Both metal ions within the binding site, Zn^{2+} and Mg^{2+} respectively, were preserved in the structures. In addition, the structural water molecules that were

coordinated with the metal ions were left in their places in the crystal structures. In the tadalafil-bound crystal structure seven water molecules were preserved for docking (waters 1001−1007). These are the same water molecules used in building the PDE-5 specific DUD set.[22] In the sildenafil-bound crystal structure fewer water molecules are originally present in the binding site, and, hence, only three water molecules were preserved (waters 45, 86, and 111). The docking was performed with GLIDE 5.5[28] using the default settings in the standard precision (SP) mode. The docking poses were validated by comparing them against the alignments seen in the inhibitor-bound PDE-5 crystal structures (Figure S1). rmsd values were calculated for tadalafil (0.2 Å) and sildenafil (1.1 Å), which shows that the docking method was able to reproduce the crystallized ligand poses for PDE5-Is. GLIDE was able to dock all active compounds but failed in docking 34 of the specific PDE-5 decoys and 269 of the other DUD decoys. These failed docking results were put into the bottom of the best-ranked list for subsequent enrichment analyses.

Molecular Dynamics Simulations. For postprocessing of the vHTS results, the top 5% of the ranked molecules were further analyzed with the MD/MMGBSA procedure to get binding free energy estimations for the quickly relaxed complexes. For this, the MD/MMGBSA algorithms distributed in the AMBER 10[27] package were used. The ligand conformation superimposed on the query molecule with SHAEP or the docking pose provided by GLIDE was used together with the protein crystal structure as a starting conformation for MD simulations. Charges for the ligands were derived with AM1-BCC[28] available in ANTECHAMBER. TLEAP in ANTECHAMBER was used to create force field parameters for the protein (ff03[29]) and the ligand (gaff[30]), add hydrogens, and solvate the ligand-protein complex with a rectangular box of transferable intermolecular potential three-point water molecules (TIP3P[31]) 4 Å in all directions. The MD simulations were run with SANDER module within AMBER 10 with the following protocol. The system was first minimized with conjugate-gradient method for 1000 steps without restraints. This was followed by an equilibration step at constant volume by allowing the system to heat from 100 to 300 K for 1000 steps with NMR restraints. The production simulation without restraints was run for 20,000 steps (simulation time 40 ps) at constant pressure controlled by isotropic position scaling. Temperature was maintained with the Berendsen thermostat,[32] applied with a heat bath coupling time of 0.2 ps. Electrostatics were treated with Particle-Mesh Ewald (PME) method,[33,34] and cutoff value of 12 Å for nonbonded interactions was employed. The equilibration step and the production simulation were run under periodic boundary conditions. The SHAKE algorithm[35] was used to restrain bonds involving hydrogen atoms, allowing the use of 2 fs time step.

Molecular Mechanics/Generalized Born Surface Area Calculations. In the MMGBSA calculations the free energy of the ligand binding is estimated by taking into account the solvation energies of the interacting molecules, in addition, to molecular mechanics (MM) energies. The contribution of polar solvation energy is calculated with generalized Born (GB) implicit solvent model; whereas the nonpolar part of the solvation energy is dependent on the solvent accessible surface area (SA). The free energies of binding (ΔG_{bind}) can be estimated from the free energies of the three reactants with the eq 1

$$\Delta G_{bind} = < G_{comp} > - < G_{rec} > - < G_{lig} > \quad (1)$$

where < > denotes an average over a set of snapshots along the MD trajectory, and comp, rec, and lig stand for complex, receptor, and ligand, respectively. The free energy for each of the reactants is estimated with the eq 2

$$G = E_{MM} + G_{solv} - TS_{solute} \quad (2)$$

where E_{MM} is the molecular mechanics contribution in vacuo consisting of the sum of internal, electrostatics, and van der Waals energies; G_{solv} is the contribution of solvation free energies expressed as the sum of polar and nonpolar solvation free energies; T is the temperature; and S_{solute} is the solute entropy.

For MMGBSA analysis, snapshots at 400 fs intervals were extracted from the MD trajectory, and the binding free energies were averaged over the ensemble of conformers produced (100 snapshots for each reactant). The atomic cavity radii and charges were taken from the corresponding topology files. The polar solvation energies were calculated with the GB approach implemented in AMBER 10. Dielectric constants of 1 and 80 were used for the interior and the exterior of the molecules, respectively. The parameters for GB calculations developed by Tsui and Case[8] were used (igb = 1). The hydrophobic contribution to the solvation free energy was estimated by calculating the solvent accessible surface area with Molsurf.[36]

The estimation of entropy is usually done with normal-mode analysis of the vibration frequencies. However, this is computationally very expensive,[37] making it unsuitable for vHTS. Thus, the effect of entropy was neglected in the calculations.

Receiver Operating Characteristic − Area under Curve and Enrichment. A summary of receiver operating characteristic (ROC) curve was given as an area under curve (AUC) value. The absolute enrichment (eq 3) of the vHTS protocols were calculated as follows

$$\text{absolute enrichment} = (\text{Ligs}_{n\%} * \text{Mols}_{\text{all}})/(\text{Mols}_{n\%} * \text{Ligs}_{\text{all}}) \quad (3)$$

where $\text{Ligs}_{n\%}$ and $\text{Mols}_{n\%}$ are the number of ligands and molecules, respectively, in the top-n% of screened compounds, and Ligs_{all} and Mols_{all} are number of ligands and molecules, respectively, in the total set of screened molecules. The maximal enrichment is solely dependent on the relation $\text{Mols}^{\text{all}}/\text{Ligs}^{\text{all}}$. Accordingly, the maximal enrichment depends on the number of used ligands and decoy molecules. Here, the maximal enrichment with the PDE-5/DUD decoys is 94.1, and with the PDE-5 decoys 36.4.

Figures 1 and 2B-D were prepared by using BODIL,[38] MOLSCRIPT v.2.1.2,[39] and RASTER3D package.[40]

RESULTS

Before implementing the novel features to the NIB or ligand-based screening we wanted to compare the methods using default settings against molecular docking. Therefore, the PDE5-Is were first searched using the ligand shape-based screening and the protein structure-based methods: molecular docking and NIB shape-based screening.

Ligand Shape-Based Screening. Neither of the PDE5-I structures (Figure 2A and B) could distinguish very effectively active molecules from the PDE-5/DUD or the PDE-5 decoys in the ligand shape-based searches (Table 1). The AUC values of sildenafil-based searches with both decoy sets were below 0.5 (Table 1), which means that randomly picked molecules should

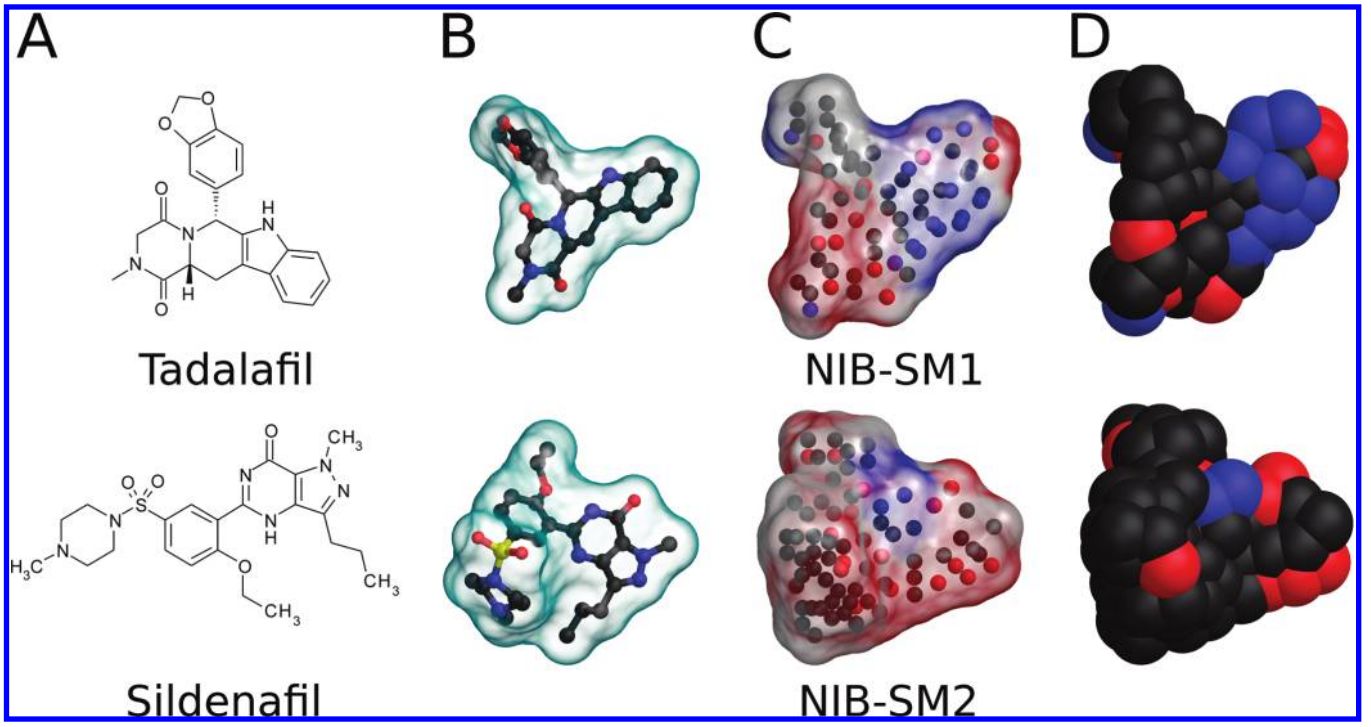

Figure 2. The PDE-5 inhibitors and negative images of the substrate-binding site. (A) The 2D and (B) the 3D structures of PDE5-Is indicate that sildenafil (down) is substantially bulkier than tadalafil (up). (C) The NIB-SM2 model (down) is also bulkier than the NIB-SM1 model (up). The dots, which are surrounded by the transparent solvent accessible surface, represent the data points used in the NIB screening. Both in the solvent-accessible surface and data points the positive and negative charges are differentiated by red and blue colors, respectively (white/black = neutral). Similarly, (D) the data points are shown using space-filling cpk models.

Table 1. ROC AUC Values for Shape-Based vHTS with PDE-5[b]

	SHAEP			
	ligand-based		NIB	
target	PDE-5/DUD	PDE-5	PDE-5/DUD	PDE-5
tadalafil/ NIB-SM1	0.58 ± 0.04	0.67 ± 0.04	**0.75 ± 0.04**	0.72 ± 0.04
sildenafil/ NIB-SM2	0.48 ± 0.04	0.42 ± 0.04	**0.71 ± 0.03**	0.65 ± 0.04
Combi[a]	0.57 ± 0.04	0.64 ± 0.04	**0.75 ± 0.04**	0.72 ± 0.04

[a] Either both tadalafil and sildenafil structures or SM1 and SM2 models were used. [b] The best enrichments are shown in bold.

contain more actives. The highest AUC value was produced by tadalafil-based search with the PDE-5 decoys (AUC = 0.67 ± 0.04; Table 1) or the PDE-5/DUD decoys (AUC = 0.58 ± 0.04; Table 1); however, these values were clearly lower than the ones produced by the protein structure-based methods (Tables 1 and 2). The combination of ligand structure data from both sildenafil and tadalafil (Figure 2B) did not improve the results but weakened them marginally with both decoy sets (Table 1). The set of active ligands used in the vHTS does not include many as bulky molecules as sildenafil, which is why the sildenafil shape-based vHTS could perform better in actual screening experiments. If only the top 0.5% of the ranked ligand shape-based results were inspected, the method found more active hits (Table 3) and produced marginally better enrichment (Table 4) than the shape-based NIB screening (see below). However, as a whole the ligand shape-based vHTS produced weaker enrichment than the protein structure-based methods.

Protein Structure-Based Screening. *Docking.* The advantage of docking is that it takes into consideration both the shape and the electrostatics of the PDE-5 substrate-binding site. The docking/scoring of GLIDE produced relatively weak enrichment when the tadalafil-PDE-5 crystal structure (PDB: 1XOZ) was utilized in the vHTS (Table 2). In contrast, with the sildenafil-bound structure (PDB: 2H42), the docking was able to find more active ligands than either the ligand shape-based or the NIB shape-based screening (Table 1) with the PDE-5 (AUC = 0.73 ± 0.04; Table 2) or the PDE-5/DUD decoys (AUC = 0.78 ± 0.04; Table 2). The preference for the sildenafil-bound structure in docking is explained by the different solvation states of the crystal structures. The use of both crystal structures in the docking screening produced the highest AUC value with the PDE-5 decoys (AUC = 0.80 ± 0.03; Table 2). The docking produced even better results with both decoy sets if the amount of active hits (Table 3) and the level of enrichment (Table 4) were inspected for the top 0.5% of the ranked molecules. As a whole the results suggest that the docking works very well with the PDE-5; on the other hand, it was perplexing that GLIDE found more active ligands from the PDE-5-specific decoy set than from the larger and more diverse PDE-5/DUD decoy set. Furthermore, the downside of docking was clearly the increased computation time if compared to the other tested vHTS methods (Table 5).

Negative Image-Based Screening. The vHTS results indicated that the shape comparison of the PDE-5 substrate-binding site (Figure 2C and D) produced a higher AUC value than the

Table 2. ROC AUC Values for PDE-5 after Addition of Electrostatics and Postprocessing with the MD/MMGBSA[b]

	GLIDE		SHAEP			
	docking		ligand-based with charges		NIB with charges	
target/method	PDE-5/DUD	PDE-5	PDE-5/DUD	PDE-5	PDE-5/DUD	PDE-5
1XOZ/tadalafil/NIB-SM1	0.59 ± 0.04	0.68 ± 0.04	0.82 ± 0.03	0.69 ± 0.04	**0.83 ± 0.02**	0.69 ± 0.04
2H42/sildenafil/NIB-SM2	**0.73 ± 0.04**	**0.78 ± 0.04**	0.41 ± 0.03	0.45 ± 0.05	0.68 ± 0.03	0.64 ± 0.04
Combi[a]	0.73 ± 0.04	0.80 ± 0.03	0.81 ± 0.03	0.69 ± 0.04	**0.83 ± 0.02**	0.70 ± 0.04
Combi MD/MMGBSA[a]	0.72 ± 0.04	**0.80 ± 0.03**	0.81 ± 0.03	0.69 ± 0.04	**0.84 ± 0.02**	0.70 ± 0.04

[a] Either both the tadalafil (PDB: 1XOZ) and the sildenafil (PDB: 2H42) ligand/protein structures or the SM1 and SM2 models were used. [b] The best enrichments are shown in bold.

Table 3. Hits Using the PDE-5/DUD and the PDE-5 Decoys[a]

	PDE-5/DUD decoys				PDE-5 decoys			
method and target	0.5%	1%	5%	10%	0.5%	1%	5%	10%
Shape only								
tadalafil	2	2	5	7	2	3	10	13
sildenafil	1	1	4	6	1	1	3	6
both ligands	2	2	5	8	2	3	10	14
NIB-SM1	1	5	12	15	1	5	12	15
NIB-SM2	1	4	9	11	2	4	9	10
both NIB models	1	5	13	16	1	5	13	15
Shape and charges								
tadalafil	3	5	17	23	2	3	10	18
sildenafil	0	0	0	0	2	3	6	10
both ligands	3	5	18	20	3	3	10	18
NIB-SM1	0	4	**19**	24	0	0	12	19
NIB-SM2	0	0	1	9	3	4	9	11
both NIB models	0	4	**19**	**25**	0	0	11	19
docking (PDB: 1XOZ)	2	2	7	12	3	4	11	16
docking (PDB: 2H42)	6	8	15	19	5	8	18	20
docking (PDB: 1XOZ, 2H42)	7	7	14	16	**7**	**9**	15	**23**
Postprocessing								
both ligands	5	7	nd	nd	3	4	nd	nd
both NIB models	**10**	**12**	nd	nd	5	7	nd	nd
docking (PDB: 1XOZ, 2H42)	1	8	nd	nd	3	8	nd	nd

[a] The best enrichments are shown in bold.

Table 4. Absolute Enrichment Using the PDE-5/DUD and the PDE-5 Decoys[a]

	PDE-5/DUD decoys				PDE-5 decoys			
method and target	0.5%	1%	5%	10%	0.5%	1%	5%	10%
Shape only								
tadalafil	8	4	2	1	8	6	4	3
sildenafil	4	2	2	1	4	2	1	1
both ligands	8	4	2	2	8	6	4	3
NIB-SM1	4	10	5	3	4	10	**5**	3
NIB-SM2	4	8	4	2	8	8	4	2
both NIB models	4	10	5	3	4	10	**5**	3
Shape and charges								
tadalafil	12	10	7	5	8	6	4	**4**
sildenafil	0	0	0	0	8	6	2	2
both ligands	12	10	7	4	12	6	4	**4**
NIB-SM1	0	8	7	5	0	0	**5**	**4**
NIB-SM2	0	0	0	2	12	8	4	2
both NIB models	0	8	7	5	0	0	4	**4**
docking (PDB: 1XOZ)	8	4	5	5	12	8	3	2
docking (PDB: 2H42)	24	16	**12**	**7**	20	16	**5**	3
docking (PDB: 1XOZ, 2H42)	27	14	11	6	**28**	**18**	**5**	3
Postprocessing								
both ligands	20	14	nd	nd	12	8	nd	nd
both NIB models	**39**	**24**	nd	nd	20	14	nd	nd
docking (PDB: 1XOZ, 2H42)	8	10	nd	nd	12	16	nd	nd

[a] The best enrichments are shown in bold.

ligand shape-based screening; however, the docking worked better (Table 1). The smaller NIB solvation model (NIB-SM1, Figure 2C and D) resembles closely the shape of tadalafil and the larger those of vardenafil and sildenafil (NIB-SM2, Figure 2C and D). The NIB-SM1 model produced a higher AUC value than the equivalent NIB-SM2 model in the vHTS (Figure 2C and D; Table 1). Both the size and the shape of the NIB-SM2 model closely resemble those of sildenafil (Figure 2C and D), and thus the model has a preference for bulkier molecules. This explains the relatively low AUC value produced by the NIB-SM2 screening (Table 1); however, it does not necessarily diminish the worth of the solvation model. In contrast to the ligand shape-based screening, the combination of the NIB-SM1 and NIB-SM2 models (Figure 2C and D) did not weaken the AUC value with either the PDE-5 or the PDE-5/DUD decoys (Table 1). The combined NIB model was able to distinguish 13 active compounds from both decoy sets, when only the top 5% of the ranked molecules were inspected (Table 3). Moreover, the best enrichment for the shape-based NIB screening (10-fold; Table 4) was achieved if only the top 1% of the NIB-SM1 model or the combined NIB model results were analyzed. The docking was able to outperform the shape-based NIB (and ligand-shape based) screening if the early enrichment was calculated using both decoy sets (Tables 3 and 4).

Electrostatic Information Improved the PDE-5 Searches. The weaker overall and top enrichment produced by the NIB and ligand shape-based screening in comparison to the docking

Table 5. CPU Requirements of the vHTS Methods

method	CPU time/ligand	CPU time/40800 ligands
Shape only		
NIB	0.2 s	13 min
ligand-based	0.1 s	7 min
Shape and charges		
NIB	0.3 s	22 min
ligand-based	0.2 s	15 min
docking	12 s	16 h
Postprocessing		
MD/MMGBSA	6 h	1400 h[a]/28,000 h

[a] Time required for the MD/MMGBSA calculations for the top 5% results (240 molecules).

(Table 4) could be explained by the polarity of PDE-5 substrate-binding site (Figure 2C and D). The next logical step was to include the electrostatic information of the substrate-binding site into the NIB screening models and partial charges for the PDE5-Is in the ligand-based screening. Accordingly, this implementation should put all three vHTS methods into the same level.

Ligand-Based Screening. Addition of electrostatic information improved the ligand-based vHTS notably (Table 1 vs Table 2). Especially the AUC value of the tadalafil-based or combined search improved significantly with the PDE-5/DUD decoys (Table 2). However, the electrostatics improved the vHTS results only marginally if the PDE-5-specific decoys were used (Table 2). The sildenafil-based searches remained futile in spite of the added electrostatic information with both decoy sets (Table 2). This suggests that the sildenafil structure (Figure 2A and B) does not contain information that could improve the ligand-based vHTS at least with the used active ligand set. As stated above, sildenafil might produce the opposite outcome, if it was used to screen through a more diverse set of compounds. The addition of electrostatics into the tadalafil-based search increased the amount of active hits (Table 3) and the early enrichment (Table 4) with both decoy sets if only the top ranked compounds were studied. The use of both PDE5-Is in the vHTS did not improve the overall (Table 2) or the early enrichment (Table 4) with the electrostatic information.

Negative Image-Based Screening. The NIB models indicate that the distribution of electrostatic information is heavily influenced both by the solvation and the properties of the amino acids lining the PDE-5 binding cavity (Figure 2C and D). The NIB-SM1 model displayed more electrostatic information than the NIB-SM2 model (Figure 2C and D). The polarity of NIB-SM1 model reflects the positioning of several water molecules in the ligand-binding cavity. The added electrostatics improved the AUC value of the NIB screening considerably (Table 2) if the results were compared to the initial shape-based vHTS (Table 1). The electrostatic information did not improve the AUC value of the NIB screening as drastically as was the case with the ligand-based vHTS using the PDE-5/DUD decoys (Table 2). Both the amount of active hits (Table 3) and the early enrichment (Table 4) benefitted from the addition of electrostatics into the NIB screening; however, at the top 0.5−1% the results actually weakened (Table 4).

Although the early enrichment produced by docking was clearly the highest (Table 4), the AUC values of the NIB and the ligand-based screening acquired using the electrostatic information were actually better with the PDE-5/DUD set. This result is encouraging as the PDE-5/DUD set is more diverse than the PDE-5-specific set. The top enrichment was effectively diminished when the electrostatic information was added to the NIB-SM2 model with the PDE-5/DUD decoys (Table 4). Unexpectedly, the NIB-SM2 model worked better than the NIB-SM1 model if the top 0.5−1% of the ranked results were examined with the specific PDE-5 decoys (Tables 3 and 4). Because the other DUD decoys might contain yet unidentified active PDE-5 compounds, the NIB-SM2 model could theoretically distinguish active PDE5-Is from the other DUD ligands. Although the shape of NIB-SM2 model alone weakened the NIB search, its electrostatic information (Figure 2C and D) did in fact improve slightly the combined NIB screening if the top 10% of the ranked results were examined (Tables 3 and 4). Therefore, the usage of multiple protein conformations, or as in this case, multiple solvation models, can potentially improve the vHTS success.

The Usefulness of the Electrostatic Component Is Target Protein Specific. We also wanted to determine the effect of electrostatic information for the vHTS using target proteins with less polar ligand-binding sites than that of the PDE-5. Accordingly, some of the ligand and NIB shape-based searches already presented in our recent study[2] (Table 6) were performed again accompanied by the electrostatic information. The addition of electrostatics into the ligand-based vHTS improved the results notably if compared to the ligand shape-based results (Table 6), similarly as seen with the PDE-5 (Table 1 vs 2; Table 4). Despite the success seen with the PDE-5, in the additional test cases, docking was less effective than the other vHTS methods without exception if the AUC values were inspected (Table 6). Nevertheless, the docking results remained at a roughly comparable level with the other tested vHTS methods, and with one estrogen receptor conformation the docking produced high early enrichment values (Table 6). The addition of electrostatic information into the NIB models produced slightly better results than was seen in previous runs performed without charges; however, the early enrichment was weakened sometimes substantially (Table 6). The weighting of electrostatic potentials gave similar results as seen with the PDE-5, i.e. the AUC values were very much alike below and around equal weighting of shape and electrostatic potentials. Progesterone receptor was a notable exception as its AUC value increased significantly (from 0.50 to 0.77; Table 6) with higher weighting of the electrostatic potential contribution (70%). The results may reflect that the receptor conformation is not optimal for a large portion of the ligands, as indicated also by our previous study,[2] and, thus, usefulness of added electrostatics for NIB screening is more case-specific than with the ligand-based method. The hydrophobicity or polarity of the target protein's ligand-binding site is likely one key factor, which determines whether the addition of electrostatics into the NIB screening produces negative or positive effects.

The Postprocessing Improved the Enrichment. Although addition of electrostatic information improved both the ligand-based and the NIB screening methods (Table 2) with only minor increase to the computation time (Table 5), we wanted to enhance the top enrichment yet further. The main concern was that the conformations of the screened compounds did not complement the PDE-5 protein structure optimally. To acquire more optimal ligand conformations in relation to the residues of the PDE-5 substrate-binding site, short MD simulations with the top 5% of ranked compounds in complex with the PDE-5 crystal structures were run. From these MD simulations, the favorability

Table 6. ROC AUC Values and Enrichment Factors for a Variety of Targets after Addition of Electrostatics[d]

			SHAEP			
target[a]		GLIDE docking	ligand-based[b]	ligand-based with charges	NIB[b]	NIB with charges
AR	AUC	0.73 ± 0.03[b]	0.80 ± 0.03	**0.87 ± 0.03**	0.84 ± 0.03	0.85 ± 0.03
	1%	12.18 (9)[b]	27.07 (20)	**29.77 (22)**	14.09 (11)	17.59 (13)
	5%	7.31 (27)[b]	**10.29 (38)**	8.66 (32)	8.12 (30)	7.58 (28)
	10%	5.14 (38)[b]	**5.82 (43)**	5.55 (41)	5.14 (38)	5.14 (38)
$ER_{agonist}$	AUC	0.81 ± 0.03 [b]	0.76 ± 0.03	0.80 ± 0.03	0.79 ± 0.03	**0.82 ± 0.03**
	1%	24.16 (16) [b]	21.14 (14)	24.16 (16)	**30.20 (20)**	16.61 (11)
	5%	10.48 (35) [b]	8.69 (29)	9.28 (31)	**11.98 (40)**	10.78 (36)
	10%	5.97 (40) [b]	5.37 (36)	5.67 (38)	**6.41 (43)**	**6.41 (43)**
$ER_{antagonist}$	AUC	0.68 ± 0.05 [b]	0.81 ± 0.04	**0.84 ± 0.04**	0.75 ± 0.05	0.76 ± 0.05
	1%	**18.44 (7)** [b]	7.90 (3)	10.54 (4)	7.90 (3)	10.54 (4)
	5%	**8.19 (16)** [b]	4.61 (9)	7.17 (14)	7.68 (15)	7.68 (15)
	10%	4.10 (16) [b]	4.10 (16)	**5.89 (23)**	4.87 (19)	4.87 (19)
GR	AUC	0.59 ± 0.03	0.61 ± 0.03	0.69 ± 0.03	**0.85 ± 0.03**	0.83 ± 0.03
	1%	10.19 (8)	**14.02 (11)**	**14.02 (11)**	11.47 (9)	11.47 (9)
	5%	3.85 (15)	**5.39 (21)**	5.13 (20)	4.62 (18)	2.82 (11)
	10%	2.44 (19)	2.95 (23)	3.59 (28)	**3.98 (31)**	3.34 (26)
MR	AUC	0.73 ± 0.05 [b]	0.79 ± 0.07	**0.91 ± 0.05**	**0.91 ± 0.05**	0.90 ± 0.06
	1%	24.45 (4) [b]	24.45 (4)	**30.56 (5)**	18.34 (3)	12.22 (2)
	5%	11.79 (9) [b]	9.17 (7)	**15.72 (12)**	10.48 (8)	7.86 (6)
	10%	6.00 (9) [b]	6.00 (9)	**8.00 (12)**	6.67 (10)	6.00 (9)
PR	AUC	0.54 ± 0.06 [b]	0.50 ± 0.06	0.59 ± 0.06	0.50 ± 0.06	[c]**0.77 ± 0.06 (0.63 ± 0.06)**
	1%	3.68 (1) [b]	7.36 (2)	3.68 (1)	**25.77 (7)**	[c]22.09 (6) (22.09 (6))
	5%	0.74 (1) [b]	2.21 (3)	3.68 (5)	**5.89 (8)**	[c]**5.89 (8) (5.89 (8))**
	10%	1.49 (4) [b]	1.12 (3)	1.86 (5)	3.35 (9)	[c]**3.72 (10) (3.72 (10))**
RXRa	AUC	0.85 ± 0.04 [b]	0.92 ± 0.04	**0.99 ± 0.01**	**0.99 ± 0.01**	**0.99 ± 0.02**
	1%	15.60 (3) [b]	26.00 (5)	20.80 (4)	**31.20 (6)**	20.80 (4)
	5%	13.14 (13) [b]	13.14 (13)	**20.22 (20)**	18.20 (18)	18.20 (18)
	10%	7.48 (15) [b]	8.45 (17)	**9.97 (20)**	**9.97 (20)**	**9.97 (20)**

[a] AR, androgen receptor (PDB: 1XQ2); ER, estrogen receptor with agonist (PDB: 1L2I) and antagonist (PDB: 3ERT); GR, glucocordicoid receptor (PDB: 1M2Z); MR, mineralocorticoid receptor (PDB: 2AA2); PR, progesterone receptor (PDB: 1SR7); RXRa, retinoic X receptor alpha (PDB: 1MVC). [b] Results previously presented in Virtanen and Pentikäinen.[2] [c] The highest AUC value was achieved with overweighting of electrostatic potentials (0.7), AUC with equal weighting of electrostatic potentials and shape (0.5:0.5) is given in parentheses. [d] The best enrichments are shown in bold, and the amounts of hits are in parentheses.

of the ligand-PDE-5 interactions was evaluated using the MMGBSA calculations to rerank the ligand-PDE-5 associations. Since the earlier studies have visualized that shorter MD simulations perform better than exhaustive ones in free energy calculations,[41,42] we deliberately used short MD simulation time (40 ps) to enable the screening of large number of compounds.

Docking-Based Screening. The docking/scoring of GLIDE produced good AUC values especially with the PDE-5 decoys (Table 2), and the very early enrichment was also excellent if compared to the NIB screening or the ligand-based screening (Table 4). The addition of electrostatics improved the other vHTS methods significantly with the PDE-5/DUD decoy set in particular, and these AUC values were better than those produced by the docking (Table 2). The postprocessing with the MD/MMGBSA protocol did not significantly improve the AUC value (Table 2) or the early enrichment of docking screening (Table 4). In fact the postprocessing of docking results caused the results to weaken considerably with both decoy sets (Tables 2-4). This weakening of the enrichment likely results from poor alignment of the docked ligands when compared to the ligand-based and the NIB screening; however, the phenomenon is difficult to validate reliably. Accordingly, these PDE-5-specific results suggest that this computationally laborious postprocessing is not sensible with the docking screening performed at least with the PDE-5 (Table 5).

Ligand-Based Screening. The AUC value does not indicate clearly that the ligand-based screening was improved at all by the postprocessing (Table 2), because only the top 5% of the compounds were rescored. Hence, the higher enrichment is better seen in ROC curves built from the top 5% of the results using both decoy sets (Figure 3). Nevertheless, the MD/MMGBSA protocol increased the relative amount of the active hits (Table 3) and improved the early enrichment considerably (Table 4) when the top 0.5−1% of the ranked compounds was inspected. With the PDE-5 decoys, the postprocessing improved the enrichment only if the top 1% of the ligand-based vHTS results with electrostatic information were studied (8-fold; Table 4). A staggering 20-fold enrichment was found if the top 0.5% of the ranked results were postprocessed with both PDE5-Is using the PDE-5/DUD decoys (Table 4). Thus, the ligand-based

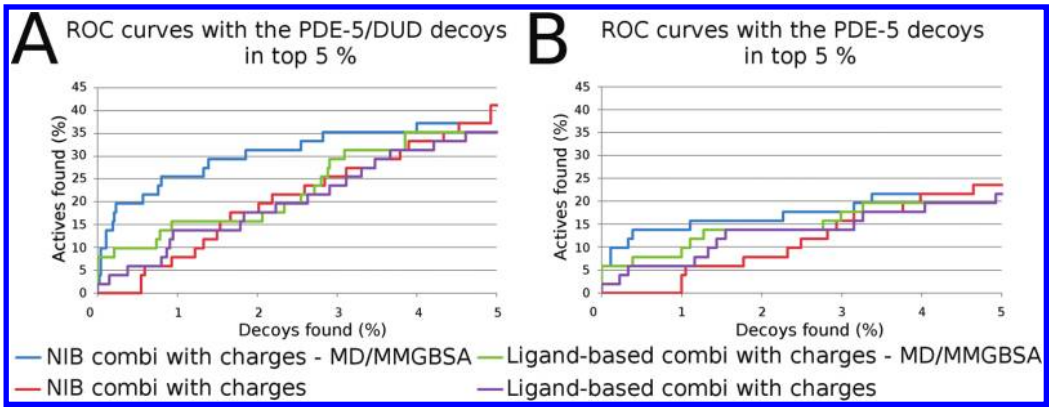

Figure 3. The receiver operating characteristic (ROC) curves in the top 5%. The ROC curves are shown with (A) the PDE-5/DUD decoys and (B) only the PDE-5 decoys. The curves include the NIB search performed with both solvation models (combi; red line) and the ligand-based search done with both tadalafil and sildenafil (combi; magenta line) using electrostatic information. These searches are also shown after postprocessing with the MD/MMGBSA protocol. Both the NIB (blue line) and ligand-based results (green line) show notable increase in the level of early enrichment after the postprocessing steps.

screening was able to find five out of 51 active ligands with the less specific PDE-5/DUD decoy set (Table 3). On the other hand, with the specific PDE-5 decoys the enrichment of the best-ranked results did not improve notably due to the postprocessing (Table 4). This shows that the MD/MMGBSA protocol can help the ligand-based vHTS in distinguishing active ligands from inactives if the properties of the decoy compounds are sufficiently different from the established active molecules.

Negative Image-Based Screening. Although the postprocessing of the NIB screening results did not significantly affect the overall AUC values (Table 2), the number of active hits (Table 3), and the top enrichment (Table 4) were greatly improved by the MD/MMGBSA treatment. The enrichment was also visible in the ROC curves of the top 5% of the results with the PDE-5/DUD (Figure 3A) and the PDE-5 decoys (Figure 3B). With the PDE-5/DUD decoys the enrichment was 39 for the top 0.5% (i.e., 20% of ligands) of the initially NIB screened results with postprocessing (Table 4) and 24 for the top 1% (Table 4). The relative enrichment was even slightly higher when using only the PDE-5 decoys (data not shown), although, numerical comparison of the absolute enrichment suggests otherwise (Table 4). Therefore, the NIB screening with electrostatics produced the highest enrichment when it was accompanied by the MD/MMGBSA protocol (Table 4). The postprocessing of the ranked NIB results produced considerably higher early enrichment than the ligand-based screening or docking. Due to the postprocessing, the NIB screening reached the level of enrichment that should reduce significantly the number of compounds that has to be tested experimentally in drug discovery projects.

DISCUSSION

Various vHTS techniques have been used to screen PDE5-Is from decoys prior to this study. Cheeseright et al. have created a novel vHTS method that generates 3D molecular field descriptors based on the query ligand, and these field points are then used in screening.[43] Kirchmair et al.[44] were able to produce first-rate enrichment in the ligand shape-based screening using several query ligands in the vHTS. A study by von Korff et al. suggests also that chemical fingerprint methods can produce very good enrichment.[45] In this study, we have continued the development of a protein structure-based vHTS method, NIB screening, which uses the negative image of the ligand-binding site of the target protein. Fundamentally, the NIB is a protein structure-based method that uses tools created for the ligand-based screening. In addition to taking into account the shape of the ligand-binding site, also protein flexibility, solvation, and electrostatic potentials can be incorporated into the NIB model. Furthermore, we show that the postprocessing of the initially ranked molecules with the MD/MMGBSA protocol produces significant early enrichment in the recognition of active ligands. Therefore, we present an alternative for previously described vHTS methods, and it should be especially useful when the number of known active ligands is low or docking is ineffective.

The AUC values indicate that in the case of PDE-5 the NIB method outperforms the ligand-based screening with or without the added electrostatics (Tables 1 and 2). This is surprising, because the PDE-5 decoys have been selected by using a ligand-based method, and thus, the set is not well suited for the evaluation of ligand-based methods.[46] On the other hand, the docking produced higher early enrichment for the PDE-5 using both decoy sets, if only 0.5% of the compounds were inspected (Table 4). Moreover, the scoring functions of the docking methods are not always able to identify active molecules with high accuracy.[1−4] This result was clearly backed up in this study by the vHTS experiments performed using a diverse set of target proteins (Table 6). Even with the PDE-5 as a target protein, the docking did not work especially well when a more diverse decoy set was utilized in the vHTS (Table 2). When electrostatic information was incorporated into the ligand-based and the NIB screening, these two methods produced roughly similar results as molecular docking. The NIB method is not especially strenuous if its computational costs are compared against the ligand-based screening or, especially, the docking (Table 5). In fact, we anticipate that when active compounds have not been detected but there exists an accurate protein structure, the NIB screening is a good alternative for the vHTS if both accuracy and speed are required.

Because the scoring functions of docking have more precise or clear-cut properties than the NIB or the ligand-based methods, it is able to find, in some cases, certain ligand conformations better than the other methods. This accuracy comes with a price, though, as only a few of the sampled ligand poses generally fulfill the strict requirements of docking scoring. Therefore, the

docking detects some of the active ligands with a high level of certainty, and this is reflected in the very early enrichment values (Tables 4 and 6) although the AUC values (Table 2) suggest much weaker enrichment in general. Moreover, it is perplexing why the enrichment produced by docking is diminished in the postprocessing stage (Table 4) although the other methods clearly benefit from the strenuous MD/MMGBSA calculations. There is at least one plausible explanation for this. If the sampled active ligands do not produce perfect matches to the surroundings, the docking algorithms usually do not rank them high. For example, the docking may have problems finding the narrow hydrophobic side pocket of the PDE-5 (Figure 1B), which is important for the subtype-specificity,[12] or, alternatively, the scoring functions do not value enough of those poses that occupy the niche. In this issue, the advantage of NIB screening is that it allows certain degree of spatial overlap between the ligand and the protein. The docking screening also produces some overlaps but nonoverlapping ligand conformations are preferred in the scoring, and, occasionally, the biologically relevant poses are ignored. In short, the NIB method gives more room to maneuver than docking.

The ligand-based screening is able to find PDE-5 specific ligands; the only requirement is that such molecules have already been established. The NIB screening circumvents this issue as prior compounds are not necessary to perform vHTS; however, a high-quality 3D structure of the target protein is required. Although the creation of a NIB model requires certain amount of expertise, it is still a fairly simple procedure. For example, the derivation of a NIB model can be difficult for the ligand-binding sites at flat surfaces formed in protein−protein interactions. The importance of water molecules has to be considered carefully on a case by case basis if the ligand-binding site of the protein is not entirely lipophilic and it contains polar groups. If the binding site is not completely enclosed, the user also has to determine where the binding site ends and the periphery begins. As the NIB screening is rapid, the importance of each data point and water molecule can be determined individually if necessary. Alternatively, numerous NIB models can be created and used simultaneously in the vHTS experiments if it produces higher enrichment than one model alone. Also the use of multiple crystal structures or MD simulation snapshots can have positive effects for the vHTS results as the ligand-binding sites can adopt very different conformations with different binding agents.[2]

The solvation and the bound ligand can affect the shape of the ligand-binding site, as is the case with the NIB-SM1 and NIB-SM2 models (Figure 2C and D) used in this study. For example, the shape of tadalafil is similar to the shape of the NIB-SM1 model (Figure 2B vs C). Because the active ligand set for the PDE-5 included compounds with similar features as tadalafil (Figure 2A), both the screening with the tadalafil and the NIB-SM1 model produced similar level of enrichment in the vHTS. This should not be interpreted to mean that different shaped NIB models would not work as well with different target proteins or in actual drug screening projects. A NIB model could be created for example based on a PDE-5 crystal structure lacking a bound molecule altogether, and there is no logical reason why it would not perform well in vHTS. In fact, different conformations of the substrate-binding site are likely needed if we are to acquire novel lead-like PDE5-Is that do not mimic the established molecules. The NIB screening should also be useful in cases where scaffold hopping is desired for intellectual property issues. The situation is similar to the ligand shape-based vHTS performed for PDE-5, which produces better enrichment if several query ligands are used.[44] Nevertheless, the negative images of PDE-5 substrate-binding site filled effectively the two hydrophobic niches involved in the PDE5-I binding (Figure 1B), which is a prerequisite to ensure PDE-5 specificity.[12] Therefore, if the NIB screening results were used in actual experimental testing, the top-ranked molecules should be PDE-5-specific.

Although the protein's electrostatic information improved the NIB screening (Table 1 vs Table 2), the effects of the charges should be studied further. Dissimilar settings are likely to describe better the electrostatic properties of the ligand-binding sites of different target proteins. Also the MD/MMGBSA protocol was proven to be a very useful tool when sorting out the active ligands from the decoy molecules (Table 2; Figure 3). The postprocessing increased the early enrichment of both the ligand-based screening and the NIB screening considerably (Table 4). Accordingly, here, only a fraction of the ranked results were re-examined with the MD/MMGBSA protocol, due to the high computational cost of this procedure (Table 5). Moreover, the NIB screening benefitted most from this additional phase as the early enrichment was highest with both used decoy sets. The results indicated that these extra computational costs to the NIB screening were compensated handsomely by the increased enrichment (Table 4).

CONCLUSIONS

This study has indicated that the NIB screening is a viable option to the other vHTS methods with the PDE-5. The results also suggest that the addition of electrostatic information into NIB screening can be useful with other target proteins. While in our previous study we noticed that the usage of multiple protein conformations enriches the identification of active ligands from inactive molecules, here, we incorporated the usage of electrostatic information and solvation into the NIB search. Thus, the simultaneous incorporation of polar interactions, solvation, and the variation in the shape of the target protein's ligand-binding site were successfully used in the vHTS. Additional postprocessing with the MD/MMGBSA protocol raised the enrichment of the NIB screening into a level that is needed to keep the costs of drug discovery projects within reasonable limits.

ASSOCIATED CONTENT

Supporting Information. The ability of the docking software to reproduce the binding poses of the sildenafil and tadalafil seen in the crystal structures was validated prior to the docking of other PDE5-Is and decoy molecules (Figure S1). This material is available free of charge via the Internet at http://pubs.acs.org.

AUTHOR INFORMATION

Corresponding Author

*Phone: +358-40-521-6913. E-mail: olli.t.pentikainen@jyu.fi.

Present Addresses

[‖]Department of Physics, P.O. Box 692, FI-33101, Tampere University of Technology, Finland.

Author Contributions

[§]These authors made equal contributions to this work.

■ ACKNOWLEDGMENT

This study was funded by the Drug Discovery Graduate School (SIV) and the National Doctoral Programme in Informational and Structural Biology (PAP). CSC - The Finnish IT Centre for Science is acknowledged for their generous computational grants (jyy2516, gc2571).

■ ABBREVIATIONS:

NIB, negative image-based; vHTS, virtual high-throughput screening; PDE-5, cyclic nucleotide phosphodiesterase type 5; PDE5-I, PDE-5 inhibitor; MD, molecular dynamics; MMGBSA, molecular mechanics-generalized Born surface area; ROC, receiver operating characteristic; AUC, area under curve; DUD, directory of useful decoys; AR, androgen receptor; ER, estrogen receptor; GR, glucocordicoid receptor; MR, mineralocorticoid receptor; PR, progesterone receptor; RXRa, retinoic X receptor alpha

■ REFERENCES

(1) Warren, G. L.; Andrews, C. W.; Capelli, A.; Clarke, B.; LaLonde, J.; Lambert, M. H.; Lindvall, M.; Nevins, N.; Semus, S. F.; Senger, S.; Tedesco, G.; Wall, I. D.; Woolven, J. M.; Peishoff, C. E.; Head, M. S. A critical assessment of docking programs and scoring functions. *J. Med. Chem.* **2006**, *49*, 5912–5931.

(2) Virtanen, S. I.; Pentikäinen, O. T. Efficient virtual screening using multiple protein conformations described as negative images of the ligand-binding site. *J. Chem. Inf. Model.* **2010**, *50*, 1005–1011.

(3) McGaughey, G. B.; Sheridan, R. P.; Bayly, C. I.; Culberson, J. C.; Kreatsoulas, C.; Lindsley, S.; Maiorov, V.; Truchon, J.; Cornell, W. D. Comparison of topological, shape, and docking methods in virtual screening. *J. Chem. Inf. Model.* **2007**, *47*, 1504–1519.

(4) Cross, J. B.; Thompson, D. C.; Rai, B. K.; Baber, J. C.; Fan, K. Y.; Hu, Y.; Humblet, C. Comparison of several molecular docking programs: pose prediction and virtual screening accuracy. *J. Chem. Inf. Model.* **2009**, *49*, 1455–1474.

(5) Yang, S. Pharmacophore modeling and applications in drug discovery: challenges and recent advances. *Drug Discovery Today* **2010**, *15*, 444–450.

(6) Lee, H. S.; Lee, C. S.; Kim, J. S.; Kim, D. H.; Choe, H. Improving virtual screening performance against conformational variations of receptors by shape matching with ligand binding pocket. *J. Chem. Inf. Model.* **2009**, *49*, 2419–2428.

(7) Ebalunode, J. O.; Ouyang, Z.; Liang, J.; Zheng, W. Novel approach to structure-based pharmacophore search using computational geometry and shape matching techniques. *J. Chem. Inf. Model.* **2008**, *48*, 889–901.

(8) Tsui, V.; Case, D. A. Molecular dynamics simulations of nucleic acids with Generalized Born solvation model. *J. Am. Chem. Soc.* **2000**, *122*, 2489–2498.

(9) Zhang, K. Y. J.; Card, G. L.; Suzuki, Y.; Artis, D. R.; Fong, D.; Gillette, S.; Hsieh, D.; Neiman, J.; West, B. L.; Zhang, C.; Milburn, M. V.; Kim, S.; Schlessinger, J.; Bollag, G. A glutamine switch mechanism for nucleotide selectivity by phosphodiesterases. *Mol. Cell* **2004**, *15*, 279–286.

(10) Wang, H.; Liu, Y.; Huai, Q.; Cai, J.; Zoraghi, R.; Francis, S. H.; Corbin, J. D.; Robinson, H.; Xin, Z.; Lin, G.; Ke, H. Multiple conformations of phosphodiesterase-5: implications for enzyme function and drug development. *J. Biol. Chem.* **2006**, *281*, 21469–21479.

(11) Chen, G.; Wang, H.; Robinson, H.; Cai, J.; Wan, Y.; Ke, H. An insight into the pharmacophores of phosphodiesterase-5 inhibitors from synthetic and crystal structural studies. *Biochem. Pharmacol.* **2008**, *75*, 1717–1728.

(12) Card, G. L.; England, B. P.; Suzuki, Y.; Fong, D.; Powell, B.; Lee, B.; Luu, C.; Tabrizizad, M.; Gillette, S.; Ibrahim, P. N.; Artis, D. R.; Bollag, G.; Milburn, M. V.; Kim, S.; Schlessinger, J.; Zhang, K. Y. J. Structural basis for the activity of drugs that inhibit phosphodiesterases. *Structure* **2004**, *12*, 2233–2247.

(13) Allerton, C. M. N.; Barber, C. G.; Beaumont, K. C.; Brown, D. G.; Cole, S. M.; Ellis, D.; Lane, C. A. L.; Maw, G. N.; Mount, N. M.; Rawson, D. J.; Robinson, C. M.; Street, S. D. A.; Summerhill, N. W. A novel series of potent and selective PDE5 inhibitors with potential for high and dose-independent oral bioavailability. *J. Med. Chem.* **2006**, *49*, 3581–3594.

(14) Hatzimouratidis, K.; Hatzichristou, D. G. A comparative review of the options for treatment of erectile dysfunction: which treatment for which patient? *Drugs* **2005**, *65*, 1621–1650.

(15) Galiè, N.; Ghofrani, H. A.; Torbicki, A.; Barst, R. J.; Rubin, L. J.; Badesch, D.; Fleming, T.; Parpia, T.; Burgess, G.; Branzi, A.; Grimminger, F.; Kurzyna, M.; Simonneau, G. Sildenafil citrate therapy for pulmonary arterial hypertension. *N. Engl. J. Med.* **2005**, *353*, 2148–2157.

(16) Katz, S. D.; Balidemaj, K.; Homma, S.; Wu, H.; Wang, J.; Maybaum, S. Acute type 5 phosphodiesterase inhibition with sildenafil enhances flow-mediated vasodilation in patients with chronic heart failure. *J. Am. Coll. Cardiol.* **2000**, *36*, 845–851.

(17) Hirata, K.; Adji, A.; Vlachopoulos, C.; O'Rourke, M. F. Effect of sildenafil on cardiac performance in patients with heart failure. *Am. J. Cardiol.* **2005**, *96*, 1436–1440.

(18) Halcox, J. P. J.; Nour, K. R. A.; Zalos, G.; Mincemoyer, R. A.; Waclawiw, M.; Rivera, C. E.; Willie, G.; Ellahham, S.; Quyyumi, A. A. The effect of sildenafil on human vascular function, platelet activation, and myocardial ischemia. *J. Am. Coll. Cardiol.* **2002**, *40*, 1232–1240.

(19) Chen, J.; Mabjeesh, N. J.; Matzkin, H.; Greenstein, A. Efficacy of sildenafil as adjuvant therapy to selective serotonin reuptake inhibitor in alleviating premature ejaculation. *Urology* **2003**, *61*, 197–200.

(20) Berman, H. M.; Westbrook, J.; Feng, Z.; Gilliland, G.; Bhat, T. N.; Weissig, H.; Shindyalov, I. N.; Bourne, P. E. The Protein Data Bank. *Nucleic Acids Res.* **2000**, *28*, 235–242.

(21) Wang, J.; Wang, W.; Kollman, P. A.; Case, D. A. Automatic atom type and bond type perception in molecular mechanical calculations. *J. Mol. Graphics Modell.* **2006**, *25*, 247–260.

(22) Huang, N.; Shoichet, B. K.; Irwin, J. J. Benchmarking sets for molecular docking. *J. Med. Chem.* **2006**, *49*, 6789–6801.

(23) Watts, K. S.; Dalal, P.; Murphy, R. B.; Sherman, W.; Friesner, R. A.; Shelley, J. C. ConfGen: a conformational search method for efficient generation of bioactive conformers. *J. Chem. Inf. Model.* **2010**, *50*, 534–546.

(24) Halgren, T. Merck molecular force field. I. Basis, form, scope, parameterization, and performance of MMFF94. *J. Comput. Chem.* **1996**, *17*, 490–519.

(25) Kleywegt, G. J.; Jones, T. A. Detection, delineation, measurement and display of cavities in macromolecular structures. *Acta Crystallogr., Sect. D: Biol. Crystallogr.* **1994**, *50*, 178–185.

(26) Vainio, M. J.; Puranen, J. S.; Johnson, M. S. ShaEP: molecular overlay based on shape and electrostatic potential. *J. Chem. Inf. Model.* **2009**, *49*, 492–502.

(27) Case, D. A.; Darden, T. A.; Cheatham, T. E. I.; Simmerling, C. L.; Wang, J.; Duke, R. E.; Luo, R.; Crowley, M.; Walker, R. C.; Zhang, W.; Merz, K. M.; Wang, B.; Hayik, S.; Roitberg, A.; Seabra, G.; Kolossváry, I.; Wong, K. F.; Paesani, F.; Vanicek, J.; Wu, X.; Brozell, S. R.; Steinbrecher, T.; Gohlke, H.; Yang, L.; Tan, C.; Mongan, J.; Hornak, V.; Cui, G.; Mathews, D. H.; Seetin, M. G.; Sagui, C.; Babin, V.; Kollman, P. A. *AMBER 10*; University of California: San Francisco, 2008.

(28) Jakalian, A.; Bush, B. L.; Jack, D. B.; Bayly, C. I. Fast, efficient generation of high-quality atomic charges. AM1-BCC model: 1. Method. *J. Comput. Chem.* **2000**, *21*, 132–141.

(29) Duan, Y.; Wu, C.; Chowdhury, S.; Lee, M. C.; Xiong, G.; Zhang, W.; Yang, R.; Cieplak, P.; Luo, R.; Lee, T.; Caldwell, J.; Wang, J.; Kollman, P. A. A point-charge force foeld for molecular mechanics simulations of proteins based on condensed-phase quantum mechanical calculations. *J. Comput. Chem.* **2003**, *21*, 1999–2012.

(30) Wang, J.; Wolf, R. M.; Caldwell, J. W.; Kollman, P. A.; Case, D. A. Development and testing of a general AMBER force field. *J. Comput. Chem.* **2004**, *25*, 1157–1174.

(31) Åqvist, J. Ion-water interaction potentials derived from free energy perturbation simulations. *J. Phys. Chem.* **1990**, *94*, 8021–8024.
(32) Berendsen, H. J. C.; Postma, J. P. M.; Van Gunsteren, W. F.; Dinola, A.; Haak, J. R. Molecular-dynamics with coupling to an external bath. *J. Chem. Phys.* **1984**, *81*, 3684–3690.
(33) Darden, T.; York, Y.; Pedersen, L. Particle mesh Ewald: An W log(N) method for Ewald sums in large systems. *J. Chem. Phys.* **1993**, *98*, 10089–10092.
(34) Petersen, A. Accuracy and efficiency of the particle mesh Ewald method. *J. Chem. Phys.* **1995**, *103*, 3668–3679.
(35) Ryckaert, J.; Ciccotti, G.; Berendsen, H. Numerical integration of the Cartesian equations of proteins and nucleic acids. *J. Comput. Phys.* **1977**, *23*, 327–341.
(36) Connolly, M. L. Analytical molecular surface calculation. *J. Appl. Crystallogr.* **1983**, *16*, 548–558.
(37) Gohlke, H.; Case, D. A. Converging free energy estimates: MM-PB(GB)SA studies on the protein-protein complex Ras-Raf. *J. Comput. Chem.* **2004**, *25*, 238–250.
(38) Lehtonen, J. V.; Still, D.; Rantanen, V.; Ekholm, J.; Björklund, D.; Iftikhar, Z.; Huhtala, M.; Repo, S.; Jussila, A.; Jaakkola, J.; Pentikäinen, O.; Nyrönen, T.; Salminen, T.; Gyllenberg, M.; Johnson, M. S. BODIL: a molecular modeling environment for structure-function analysis and drug design. *J. Comput.-Aided Mol. Des.* **2004**, *18*, 401–419.
(39) Kraulis, P. MOLSCRIPT: A Program to Produce Both Detailed and Schematic Plots of Protein Structures. *J. Appl. Crystallogr.* **1991**, *24*, 946–950.
(40) Merritt, E. A.; Bacon, D. J. Raster3D: photorealistic molecular graphics. *Methods Enzymol.* **1997**, *277*, 505–524.
(41) Kuhn, B.; Gerber, P.; Schulz-Gasch, T.; Stahl, M. Validation and use of the MM-PBSA approach for drug discovery. *J. Med. Chem.* **2005**, *48*, 4040–4048.
(42) Ferrari, A. M.; Degliesposti, G.; Sgobba, M.; Rastelli, G. Validation of an automated procedure for the prediction of relative free energies of binding on a set of aldose reductase inhibitors. *Bioorg. Med. Chem.* **2007**, *15*, 7865–7877.
(43) Cheeseright, T. J.; Mackey, M. D.; Melville, J. L.; Vinter, J. G. FieldScreen: virtual screening using molecular fields. Application to the DUD data set. *J. Chem. Inf. Model.* **2008**, *48*, 2108–2117.
(44) Kirchmair, J.; Distinto, S.; Markt, P.; Schuster, D.; Spitzer, G. M.; Liedl, K. R.; Wolber, G. How to optimize shape-based virtual screening: choosing the right query and including chemical information. *J. Chem. Inf. Model.* **2009**, *49*, 678–692.
(45) von Korff, M.; Freyss, J.; Sander, T. Comparison of ligand- and structure-based virtual screening on the DUD data set. *J. Chem. Inf. Model.* **2009**, *49*, 209–231.
(46) Irwin, J. J. Community benchmarks for virtual screening. *J. Comput.-Aided Mol. Des.* **2008**, *22*, 193–199.